

# Synthesis and study of radical cation salts and TCNQ charge transfer complexes of a series of tetrathiafulvalenes (TTF) substituted by one or two hydroxylated side chain(s): –SCH<sub>2</sub>CH<sub>2</sub>OH<sup>†</sup>

Jean-Pierre Legros,<sup>a</sup> Françoise Dahan,<sup>a</sup> Laurent Binet,<sup>b</sup> Carole Carcel<sup>b</sup> and Jean-Marc Fabre<sup>\*b</sup>

<sup>a</sup>Laboratoire de Chimie de Coordination, CNRS-UPR 8241, 205 route de Narbonne, F 31077 Toulouse cedex-4, France

<sup>b</sup>Laboratoire de Chimie Organique: Hétérochimie et Matériaux Organiques, ENSCM-ESA 5076, 8 rue de l'École Normale, F 34296 Montpellier cedex-5, France

Received 14th April 2000, Accepted 19th September 2000

First published as an Advance Article on the web 6th November 2000

Unsymmetrically substituted tetrathiafulvalene derivatives containing hydroxy group(s) on side-chain(s) have been synthesized from cyano precursors *via* either a cross-coupling reaction or a Wittig-type condensation. As deduced from cyclic voltammetry data, the electron donor properties of the obtained compounds have been found to be similar to those of BEDTTTF. A series of radical cation salts derived from these donors has been obtained by electrocrystallization and charge transfer complexes have been prepared chemically by using TCNQ as an electron acceptor. The electrical conductivity of these phases ranges from  $3 \times 10^{-2}$  to  $7 \times 10^{-7}$  S cm<sup>-1</sup> which is consistent with their structural features. X-Ray structural analysis of three of the radical cation salts with monovalent closed-shell anions (Br<sup>-</sup>, ClO<sub>4</sub><sup>-</sup>) indicates a 1:1 stoichiometry which implies that, in each case, the donor has been oxidized to the D<sup>+</sup> state. In the same way, a crystal structure made of stacks where the donor and the acceptor molecules alternate has been found for a charge transfer complex between TCNQ and a donor derived from EDTTTF. The crystal structure of one of the donors indicates that the flexibility of the hydroxylated side chains appears as a favourable feature for the formation of hydrogen bonds.

## Introduction

In the field of molecular materials, a wide range of radical cation salts based on TTF derivatives are known as superconducting materials.<sup>1</sup> However, this remarkable electrical property has often been found to be inhibited by the occurrence of anion disorder in these salts.<sup>2</sup> In order to overcome this drawback, attempts have been made to generate hydrogen bonds between functionalized TTF's and anions in the crystalline salts<sup>3,4</sup> and between adjacent TTF units in the network. In this paper, we report on the synthesis, the electrochemical characterization and the crystal structure of unsymmetrically substituted tetrathiafulvalenes which contain hydroxy group(s) on side chain(s) liable to induce hydrogen bonds to the anions in the resulting salts. Radical cation salts with some closed shell anions and charge transfer complexes with TCNQ have been prepared by electrocrystallization and chemical redox reactions respectively. Both their electrical conductivity and their detailed crystal structure (whenever possible) are presented and discussed.

## Experimental

### Synthesis

The bis- and mono-hydroxylated tetrathiafulvalenes **2a**, **2b** and **4a**, **4b** respectively, have been prepared as shown in Scheme 1 from the key cyano derivatives **1a** and **1b**<sup>5,6</sup> obtained *via* either

a cross-coupling reaction (route a) and/or a Wittig-type reaction (route b) as already described in the literature.<sup>6,7</sup>

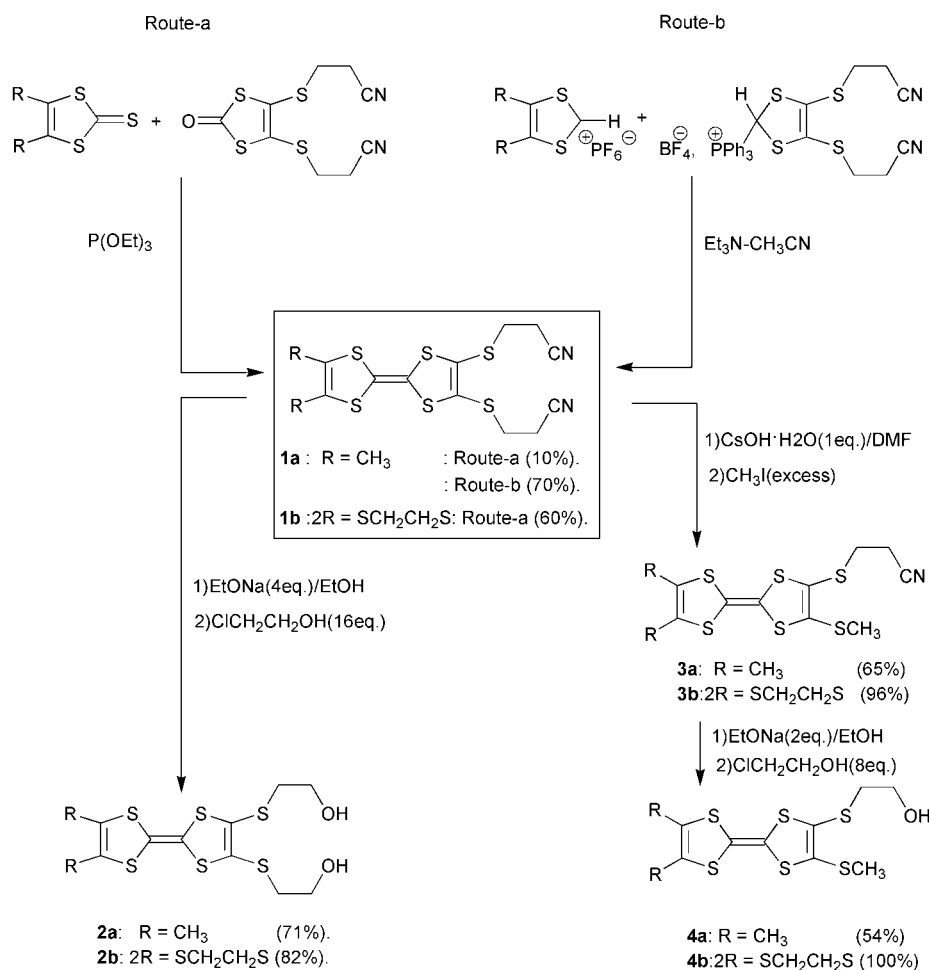
The 4,5-bis(2-hydroxyethylthio)-4',5'-dimethyltetrathiafulvalene **2a**<sup>†</sup> (also referred to as DHET-DMTTF) and the 4,5-bis(2-hydroxyethylthio)-4',5'-ethylenedithiotetrathiafulvalene **2b**<sup>6</sup> (also referred to as DHET-EDTTTF), have been directly obtained in 71% and 82% yield respectively, by thiolate deprotection of the corresponding precursor **1a** or **1b** with sodium ethoxide in ethanol followed by treatment with 2-chloroethanol<sup>5-7</sup> (*vide infra*). Similarly, the 4-(2-hydroxyethylthio)-5-methylthio-4',5'-dimethyltetrathiafulvalene **4a**<sup>8</sup> (also referred to as HETMT-DMTTF) and the 4-(2-hydroxyethylthio)-5-methylthio-4',5'-ethylenedithiotetrathiafulvalene **4b**<sup>8</sup> (also referred to as HETMT-EDTTTF), have been synthesized in 54 and 100% yield respectively, from the appropriate intermediate **3a** or **3b** by the thiolate deprotection-alkylation procedure described below. Derivatives **3a** and **3b** have been previously obtained (**3a**: 65% yield; **3b**: 96% yield) by monothiolate deprotection in the presence of caesium hydroxide monohydrate, followed by methylation with iodomethane.<sup>5,8</sup>

### Thiolate deprotection-alkylation procedure

A solution of Na (0.072 g, 3.0 mmol) in EtOH (6 mL) was added with a syringe to a suspension of the appropriate cyano derivative **1** (0.75 mmol) or **3** (1.5 mmol) in anhydrous degassed EtOH (20 mL) under N<sub>2</sub>. After being stirred at room temperature for 4 hours, the mixture was treated with 2-

<sup>†</sup>Crystal data and structure determination details for **2a** are available as supplementary data. For direct electronic access see <http://www.rsc.org/suppdata/jm/b0/b003009k/>

<sup>‡</sup>Compounds **2a**, **b** and **4a**, **b** have also been named as 2,3,6,7-tetrasubstituted tetrathiafulvalenes.



**Scheme 1**

chloroethanol (0.97 g, 12 mmol), stirred overnight, then treated with water (15 mL) and extracted with CH<sub>2</sub>Cl<sub>2</sub>. The extract was washed with water, dried over MgSO<sub>4</sub> and concentrated. The resulting solid was chromatographed [SiO<sub>2</sub>, CH<sub>2</sub>Cl<sub>2</sub>-AcOEt (8:2)] to give compounds **2** or **4**.

**Compound 2a.** (67% yield), orange powder, mp 153–154 °C. Anal. (%) calc. for C<sub>12</sub>H<sub>16</sub>O<sub>2</sub>S<sub>6</sub>: C, 37.5; H, 4.2; found: C, 37.9; H, 4.4. For spectroscopic data see ref. 7.

**Compound 2b.** (82% yield), orange powder, mp 103–104 °C. Anal. (%) calc. for C<sub>12</sub>H<sub>14</sub>O<sub>2</sub>S<sub>8</sub>: C, 32.3; H, 3.1; O, 7.2; found: C, 32.5; H, 3.0; O, 7.4. For spectroscopic data see ref. 6.

**Compound 4a.** (54% yield), orange powder, mp 86–87 °C. Anal. (%) calc. for C<sub>11</sub>H<sub>14</sub>OS<sub>6</sub>: C, 37.3; H, 4.0; O, 4.5; found: C, 37.6; H, 4.3; O, 4.6. For spectroscopic data see ref. 8.

**Compound 4b.** (100% yield), red powder, mp 80–81 °C. Anal. (%) calc. for C<sub>11</sub>H<sub>12</sub>OS<sub>8</sub>: C, 31.7; H, 2.9; O, 3.8; found: C, 31.9; H, 3.1; O, 3.8. For spectroscopic data see ref. 8.

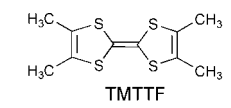
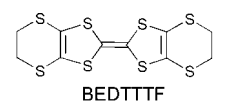
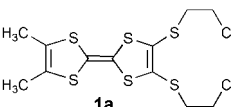
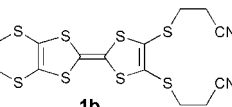
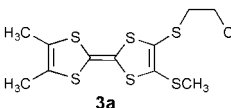
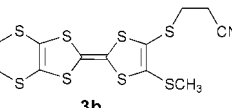
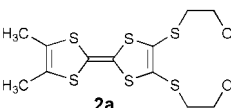
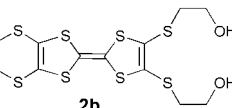
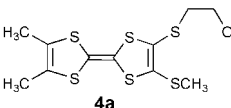
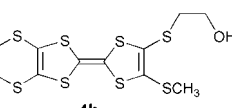
### Electrochemistry

The redox potentials of compounds **1** to **4** (10<sup>-3</sup> M) and those of TMTTF (tetramethyltetrathiafulvalene) and BEDTTTF [bis(ethylenedithio)tetrathiafulvalene], taken as references, were determined by cyclic voltammetry. Measurements were performed on platinum electrodes *versus* SCE at room temperature with tetrabutylammonium hexafluorophosphate (NBu<sub>4</sub>PF<sub>6</sub>, 0.1 M) as supporting electrolyte. A scan rate of

200 mV s<sup>-1</sup> was used. In each case, the two standard one electron reversible oxidation waves were observed. They correspond to the successive reversible formations of the radical cation (TTF<sup>•+</sup>) and dication (TTF<sup>2+</sup>) of the TTF studied. The half-wave potentials of compounds **1** to **4** were calculated from the voltammograms and reported in Table 1. These results show that the presence of the nitrile –CN and alcohol –OH functions relatively far away from the TTF core on the side chains –SCH<sub>2</sub>CH<sub>2</sub>CN and –SCH<sub>2</sub>CH<sub>2</sub>OH respectively, has only a very weak influence on the values of the half wave potentials of compounds **1** to **4**. Therefore the attracting inductive effect of these side chains corresponds approximately to that observed for thioalkyl substituents such as –SCH<sub>2</sub>CH<sub>2</sub>S– encountered in BEDTTTF. This is particularly well illustrated by compound **1b** which displays a potential ( $E_{1/2}^1 = 0.60$  V) very close to that of BEDTTTF ( $E_{1/2}^1 = 0.59$  V). Of course by decreasing the number of cyano substituents –CN or replacing it by a hydroxy group –OH less electro-attracting than –CN, the half-wave potential of the TTF decreases as observed for compounds **3b** and **2b**, **4b** respectively. It is also noteworthy that the thioalkyl group –SCH<sub>3</sub> exerts the same withdrawing effect as the –SCH<sub>2</sub>CH<sub>2</sub>OH chain as indicated through the  $E_{1/2}^1$  values observed for **2b** ( $E_{1/2}^1 = 0.54$  V) and **4b** ( $E_{1/2}^1 = 0.55$  V) respectively. The same kind of observations can be made about the series of compounds **1a** to **4a**. Nevertheless in this series, TMTTF appears, as expected, a better electron donor (lower  $E_{1/2}^1$  value: 0.28 V) than **1a**, **3a**, **2a** and **4a** (higher  $E_{1/2}^1$  values: 0.44–0.48 V) owing to the well known donating effect exerted by the methyl substituents.

A series of radical cation salts derived from **2a–b** and **4a–b** have been prepared as reported in literature,<sup>7,9</sup> by galvanostatic

**Table 1** Half-wave potentials  $E_{1/2}/V$  of TTF **1** to **4**

	0.28	0.82		0.59	1.00
	0.48	0.92		0.60	0.98
	0.47	0.93		0.56	0.95
	0.44	0.84		0.54	0.89
	0.44	0.85		0.55	0.91

electrocrystallization<sup>10</sup> ( $i \approx 1\text{--}2 \mu\text{A}$ ) on platinum electrodes in 0.05 M ( $\text{NBu}_4\text{X-CH}_3\text{OH}$ ) solutions ( $\text{X} = \text{AuBr}_2^-, \text{Br}^-, \text{Cl}^-, \text{I}_3^-, \text{ClO}_4^-, \text{NO}_3^-, \text{CF}_3\text{SO}_3^-$ ). Unexpectedly, the (**2a**- $\text{AuBr}_2$ ) salt has finally been identified (from X-ray structure determination) as the bromide salt. In addition, charge transfer complexes using TCNQ as an electron acceptor have been prepared chemically by mixing hot acetonitrile solutions containing the electron donor TTF and the electron acceptor TCNQ respectively.

### Electrical measurements

Conductivity measurements at room temperature have been carried out by the two-probe method on single or pseudo-single crystals, and, in some cases, on powder compressed pellets. The results are reported in Table 2.

### X-Ray diffraction

Most of the crystals collected on the anode of the electrocrystallization cell were twinned and of very poor quality. However, some crystals could be used for X-ray structure determinations of **2a**, the **2a**- $\text{Br}^-$  salt (hereafter **6**), the charge transfer complex **2a**-TCNQ (hereafter **8**), two different phases of the **4b**- $\text{ClO}_4^-$  salt (hereafter **9** and **9'**) and the charge transfer complex **4b**-TCNQ (hereafter **11**). The crystal structure of **8** has been published elsewhere;<sup>7</sup> the other crystal structures are described and discussed in this paper.

Data were collected at room temperature with graphite-monochromated Mo-K $\alpha$  radiation ( $\lambda = 0.71069 \text{ \AA}$ ). Crystal data and relevant data collection and refinement parameters are listed in Table 3. Intensity data reduction, structure solution and refinement were performed using standard procedures.<sup>11-14</sup>

All non-hydrogen atoms were refined anisotropically; hydrogen atoms were located on difference-Fourier maps and their contributions were included in structure factor

calculations using calculated positions and the riding model with isotropic temperature factors (not refined). However, for **2a**, all non-hydrogen atoms were refined isotropically because of the small number of observed reflections and of the poor quality of the crystal. For **6**, the positional and isotropic thermal parameters of the hydrogen atoms H(1) and H(2), which are bonded to oxygen atoms and involved in hydrogen

**Table 2** Characteristics of radical cation salts and charge transfer complexes of **2** and **4** [crystal shape, stoichiometry (cation:anion), electrical conductivity at room temperature ( $\text{S cm}^{-1}$ ), numbering]

<b>2a</b>	$\text{Cl}^-$ Platelets	$\text{Br}^-$ Small platelets	$\text{I}_3^-$ Blocks	—	TCNQ Needles
	2:1 <sup>a</sup> $3 \times 10^{-4}$	1:1 <sup>b</sup> $5 \times 10^{-4}$	— $4 \times 10^{-4}$	— $7$	2:1 <sup>b</sup> $2 \times 10^{-4}$
	<b>5</b>	<b>6</b>	<b>7</b>	<b>8</b>	<b>8</b>
<b>4b</b>	$\text{ClO}_4^-$ Blocks and square plates	$\text{ReO}_4^-$ Needles	—	—	TCNQ Needles
	1:1 <sup>b</sup> $10^{-6}$ <b>9+9'</b>	2:1 <sup>a</sup> $5 \times 10^{-5}$ <b>10</b>	—	—	1:1 <sup>b</sup> $3 \times 10^{-6}$ <b>11</b>
<b>2b</b>	$\text{ClO}_4^-$ (THF) Fine needles	$\text{Cl}^-$ Platelets	$\text{Br}^-$ Needles	$\text{CF}_3\text{SO}_3^-$ Fine needles	$\text{NO}_3^-$ Needles
	2:1 <sup>a</sup> $2 \times 10^{-3}$ <b>12</b>	2:1 <sup>a</sup> $3 \times 10^{-2}$ <b>13</b>	— $5 \times 10^{-4}$ <b>14</b>	2:1 <sup>a</sup> $7 \times 10^{-2}$ <b>15</b>	2:1 <sup>a</sup> $5 \times 10^{-4}$ <b>16</b>
	$\text{Br}^-$ Needles	$\text{I}_3^-$ Powder	—	—	TCNQ Needles
<b>4a</b>	$5 \times 10^{-7}$ <b>19</b>	$5 \times 10^{-3}$ <b>20</b>	—	—	$3 \times 10^{-2}$ <b>21</b>

<sup>a</sup>From elemental analysis. <sup>b</sup>From X-ray diffraction analysis.

**Table 3** Crystal data and structure determination details for **2a**, **6**, **9**, **9'** and **11**

Compound	<b>2a</b>	<b>6</b>	<b>9</b>	<b>9'</b>	<b>11</b>
Formula	C <sub>12</sub> H <sub>16</sub> O <sub>2</sub> S <sub>6</sub>	C <sub>12</sub> H <sub>16</sub> BrO <sub>2</sub> S <sub>6</sub>	C <sub>11</sub> H <sub>12</sub> ClO <sub>5</sub> S <sub>8</sub>	C <sub>11</sub> H <sub>12</sub> ClO <sub>5</sub> S <sub>8</sub>	C <sub>23</sub> H <sub>16</sub> N <sub>4</sub> OS <sub>8</sub>
<i>M</i>	384.6	464.5	516.1	516.1	620.9
Crystal system	Orthorhombic	Monoclinic	Monoclinic	Monoclinic	Monoclinic
Space group	<i>P</i> 2 <sub>1</sub> 2 <sub>1</sub> 2 <sub>1</sub>	<i>P</i> 2 <sub>1</sub> / <i>c</i>	<i>P</i> 2 <sub>1</sub> / <i>c</i>	<i>P</i> 2 <sub>1</sub> / <i>n</i>	<i>P</i> 2 <sub>1</sub> / <i>n</i>
<i>a</i> /Å	8.749(1)	7.517(1)	9.479(5)	20.022(4)	10.829(2)
<i>b</i> /Å	10.138(1)	19.197(2)	22.500(5)	11.553(2)	28.400(4)
<i>c</i> /Å	38.407(7)	12.574(2)	9.040(3)	8.269(2)	8.664(2)
$\beta$ /°	90	103.51(1)	92.90(3)	98.03(2)	92.72(2)
<i>V</i> /Å <sup>3</sup>	3407(1)	1764.3(1)	1926(1)	1893.9(6)	2661.5(8)
<i>Z</i>	8	4	4	4	4
$\mu$ /mm <sup>-1</sup>	0.77	2.99	1.09	1.11	0.70
Measured/independent refl. ( <i>R</i> <sub>int</sub> )	18123/2771 (0.070)	3738/3457 (0.011)	4980/2360 (0.031)	3181/2962 (0.023)	4450/4156 (0.019)
Observed refl. used for refinement	1126	1860	1663	1767	2303
<i>R</i> ( <i>F</i> ) <sup>a</sup>	0.060	0.029	0.035	0.033	0.034
<i>R</i> <sub>w</sub> ( <i>F</i> ) <sup>b</sup>	0.063	0.032	0.074	0.057	0.069

$$^a R(F) = \frac{\sum ||F_o| - |F_c||}{\sum |F_o|}, \quad ^b R_w(F) = \left[ \frac{\sum w(F_o - F_c)^2}{\sum w(F_o)^2} \right]^{1/2}.$$

bonding, were refined. For **9**, the ethylenic carbon atoms C(5) and C(6) are disordered and were refined using the occupancy factor ratio 65 : 35.

## Results and discussion

For all crystal structures relevant bond lengths and angles are given in Table 4; atoms are numbered according to Fig. 1.

Compound **2a** – The asymmetric unit contains two crystallographically independent molecules **A** and **B** of DHET-DMTTF. The two molecules **A** and **B** differ from each other in the geometry of the flexible moieties –SCH<sub>2</sub>CH<sub>2</sub>OH.

For instance, intramolecular distances between the two terminal oxygen atoms are O(1)⋯O(2) = 2.76 Å and O(21)⋯O(22) = 5.45 Å; the difference in geometry can be quantitatively expressed by the values of the torsion angles listed in Table 5. The mean planes of the TTF cores of the two molecules **A** and **B** are nearly perpendicular. Surprisingly these TTF cores are not planar: the two five membered rings make an angle of 160° in molecule **A** [containing S(1), S(2), S(3), S(4)] and 154° in molecule **B** [containing S(21), S(22), S(23), S(24)]. In the crystal structure the molecules are probably linked by a network of hydrogen bonds; however, the hydrogen atoms of the –OH groups could not be located so that one can only

**Table 4** Selected interatomic distances (Å) and bond angles (°) for **2a**, **6**, **9**, **9'** and **11** (esd's in parentheses). This table is restricted to the outmost atoms of the donor molecules (see Fig. 1 for numbering)

Distances	<b>2a</b> (mol. A)	<b>2a</b> (mol. B) <sup>a</sup>	<b>6</b>	<b>9</b> <sup>b</sup>	<b>9'</b>	<b>11</b>
S(5)–C(5)				1.812(8)	1.790(4)	1.818(5)
S(6)–C(6)				1.786(7)	1.785(4)	1.789(6)
S(7)–C(9)	1.76(3)	1.83(3)	1.813(5)	1.788(6)	1.816(4)	1.812(5)
S(8)–C(11)	1.75(3)	1.82(3)	1.811(5)	1.808(6)	1.793(5)	1.736(6)
C(5)–C(6)				1.505(8)	1.488(6)	1.472(8)
C(9)–C(10)	1.51(4)	1.35(4)	1.503(8)	1.444(8)	1.461(6)	1.520(7)
C(10)–O(1)	1.41(3)	1.45(3)	1.410(7)	1.418(7)	1.421(5)	1.390(6)
C(11)–C(12)	1.55(4)	1.52(4)	1.509(7)			
C(12)–O(2)	1.45(3)	1.39(3)	1.404(7)			

Angles	<b>2a</b> (mol. A)	<b>2a</b> (mol. B) <sup>a</sup>	<b>6</b>	<b>9</b> <sup>b</sup>	<b>9'</b>	<b>11</b>
C(3)–S(5)–C(5)	—	—	—	99.1(4)	101.4(2)	99.5(3)
C(4)–S(6)–C(6)	—	—	—	103.0(4)	101.3(2)	103.1(2)
C(1)–S(7)–C(9)	102.3(13)	100.0(13)	104.8(2)	102.9(2)	101.9(2)	100.4(2)
C(2)–S(8)–C(11)	102.4(12)	101.3(12)	103.9(2)	103.1(3)	104.2(2)	100.5(3)
S(5)–C(5)–C(6)	—	—	—	115.9(7)	116.7(4)	113.9(4)
S(6)–C(6)–C(5)	—	—	—	111.1(7)	114.7(3)	113.4(4)
S(7)–C(9)–C(10)	117.5(20)	115.9(26)	113.4(4)	111.6(5)	108.9(3)	112.5(4)
O(1)–C(10)–C(9)	111.0(22)	112.6(29)	112.2(5)	109.3(5)	112.6(4)	114.5(5)
S(8)–C(11)–C(12)	117.3(22)	111.2(21)	106.7(4)	—	—	—
O(2)–C(12)–C(11)	111.4(24)	109.0(23)	109.8(5)	—	—	—

<sup>a</sup>For atoms of molecule B, add 20 to the current numbering. <sup>b</sup>Disordered atoms: S(5)–C(5') 1.793(10); S(6)–C(6') 1.801(10); C(5')–C(6') 1.507(10); C(3)–S(5)–C(5') 108.3(7); C(4)–S(6)–C(6') 95.5(8); S(5)–C(5')–C(6') 104.4(13); S(6)–C(6')–C(5') 127(2).

**Table 5** Torsion angles in **2a**, **6**, **9**, **9'** and **11**. A positive rotation is anti-clockwise from atom 1 to atom 4, when viewed from atom 3 to atom 2

Torsion angles (°)	<b>2a</b> (A)	<b>2a</b> (B) <sup>a</sup>	<b>6</b>	<b>9</b>	<b>9'</b>	<b>11</b>
C(1)–S(7)–C(9)–C(10)	–86.3	68.4	–99.0	–129.8	–174.8	–62.8
S(7)–C(9)–C(10)–O(1)	63.8	–175.2	65.3	–53.8	–65.3	–60.8
C(2)–S(8)–C(11)–C(12)	60.2	–70.1	–172.8	—	—	—
S(8)–C(11)–C(12)–O(2)	56.4	–72.0	–58.5	—	—	—

<sup>a</sup>Add 20 to the numbering of atoms.

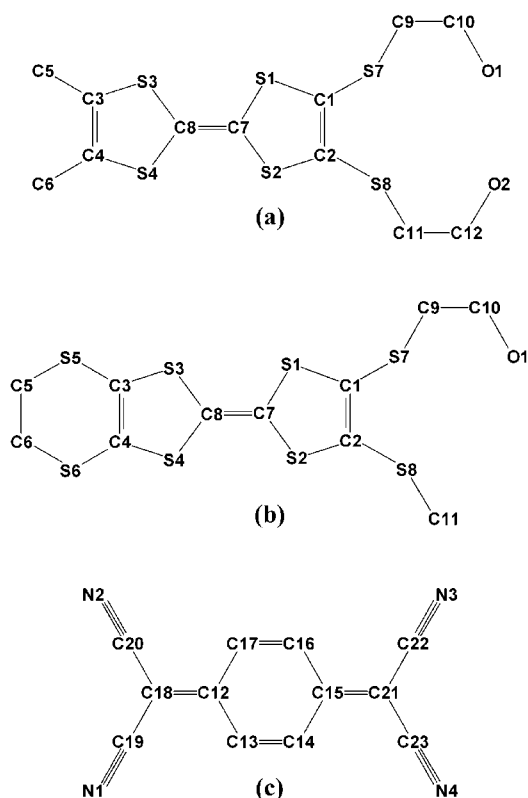


**Fig. 1** Numbering scheme of atoms used throughout the X-ray study: (a) for DHET-DMTTF in **2a** and **6** (for molecule **B** of **2a**, add 20 to this numbering); (b) for HETMT-EDTTTTF in **9**, **9'** and **11**; (c) for TCNQ in **11**.

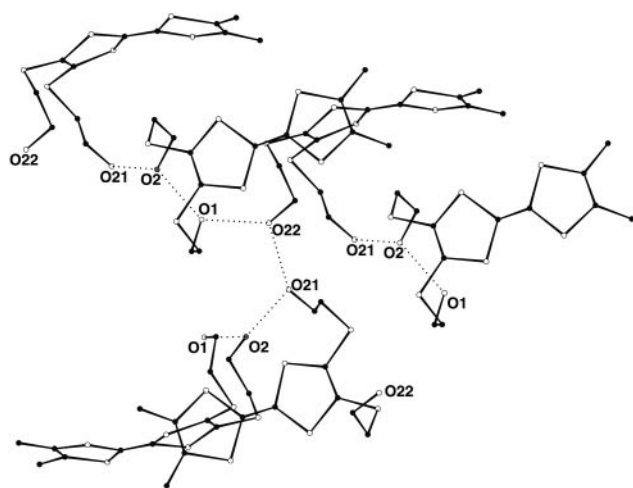


**Fig. 2** Crystal structure of **2a** showing the hydrogen bonds (dotted lines). In this and other subsequent figures, carbon atoms are drawn as black circles and non-carbon atoms are drawn as open circles.

discuss on the basis of the  $O\cdots O$  distances. The following distances ( $<3 \text{ \AA}$ ) are observed:  $O(1)\cdots O(2) = 2.762 \text{ \AA}$ ,  $O(1)\cdots O(22)^i = 2.756 \text{ \AA}$ ,  $O(2)\cdots O(21) = 2.691 \text{ \AA}$ ,  $O(21)\cdots O(22)^{ii} = 2.715 \text{ \AA}$ , where superscripts <sup>i</sup> and <sup>ii</sup> refer to the transformations  $(x, y-1, z)$  and  $(1/2+x, 3/2-y, -z)$  respectively. Assuming that these interactions correspond to hydrogen bonds, the structure can be described as made of columns of alternating perpendicular molecules, the columns being linked together by the network of hydrogen bonds as shown in Fig. 2.

**Salt 6** – The asymmetric unit contains one molecule of DHET-DMTTF and one  $\text{Br}^-$  anion, this implies that the donor is oxidized as  $(\text{DHET-DMTTF})^{\cdot+}$ . This integer

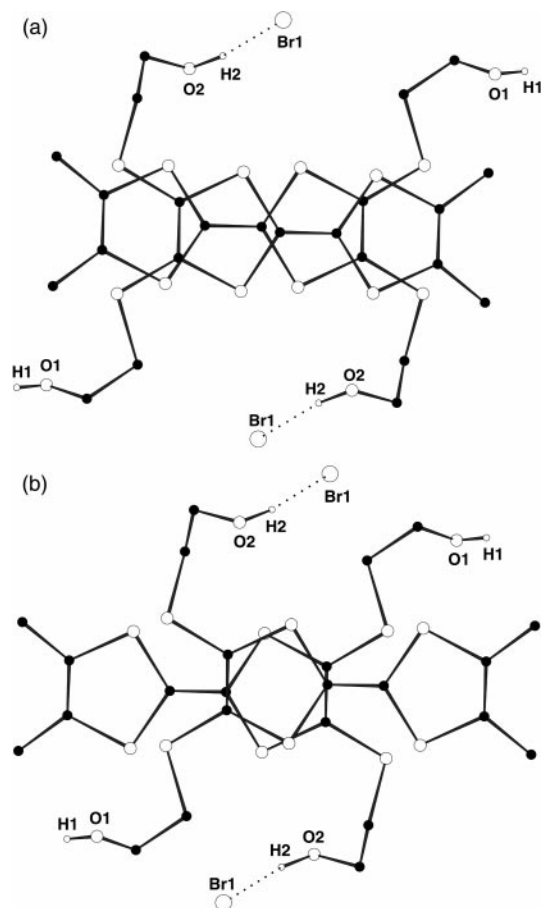


**Fig. 3** Overlapping of the DHET-DMTTF entities in **6** (a) within a dimer and (b) between two dimers (projection onto a plane parallel to the molecular plane).

oxidation state explains the low conductivity of the material (*vide supra*). Again the DHET-DMTTF unit displays a different conformation as indicated by the torsion angles of the side chains (Table 5) and the resulting intramolecular distance between the two terminal oxygen atoms  $O(1)\cdots O(2) = 8.48 \text{ \AA}$ . The donor molecules are arranged head-to-tail to form centrosymmetric dimers in which the molecules overlap in a bond-over-ring manner (Fig. 3a). These dimers pile up along the  $[100]$  direction, the molecular overlap of two adjacent dimers is of the ring-over-ring type (Fig. 3b).

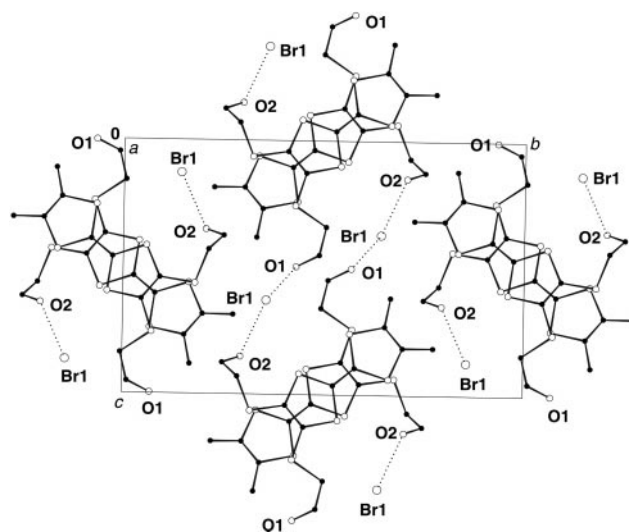


**Fig. 4** Projection of the crystal structure of **6** along  $[100]$ . Hydrogen atoms omitted for clarity.

**Table 6** Parameters (distances in Å, angles in degrees) of hydrogen bonds in **6**, **9**, **9'** and **11**

	D	H	D–H	A	H···A	D···A	D–H···A
<b>6</b>	O(1)	H(1)	1.04	Br	2.18	3.213	171
	O(2)	H(2)	0.76	Br <sup>i</sup>	2.51	3.242	162
<b>9</b>	O(1)	H(1)	0.82	O(2)	2.16	2.943	161
<b>9'</b>	O(1)	H(1)	0.82	O(2)	2.27	3.015	151
				O(3)	2.48	3.214	150
<b>11</b>	O(1)	H(1)	0.82	O(1) <sup>ii</sup>	2.51	2.907	111

<sup>i</sup>Superscripts refer to the following symmetry operators: i:  $x, y, 1+z$ ; ii:  $1-x, 1-y, 1-z$ .

The intra- and inter-dimer distances, calculated as the distances between the mean planes through the central TTF cores  $S_4C_6$ , are 3.619 and 3.558 Å respectively (note that in this discussion the notion of dimer is based on the best apparent molecular overlap so that the interplanar intra-dimer distance is larger than the inter-dimer one).

Along the [001] direction, two parallel stacks related by the crystallographic period  $c$  are linked together by hydrogen bonds involving the  $Br^-$  anions and the terminal –OH groups of the donor molecules (Fig. 4); each  $Br^-$  anion takes part in two non-equivalent hydrogen bonds (Table 6). The molecular

axes of the DHET-DMTTF entities of two adjacent stacks along the [011] direction are perpendicular to each other (Fig. 4); this arrangement prevents the formation of hydrogen bonds between adjacent stacks along the [011] direction.

Salts **9** and **9'** – Electrocrystallization of HETMT-EDTTTF with  $ClO_4^-$  as counter-anion gave batches of solids in which two kinds of crystals could be sorted on the basis of their shape: square platelets **9** and blocks **9'**. Both kinds have 1:1 stoichiometry and thus the HETMT-EDTTTF species are oxidized to monocationic state. This feature explains the low conductivity measured at room temperature. Both phases

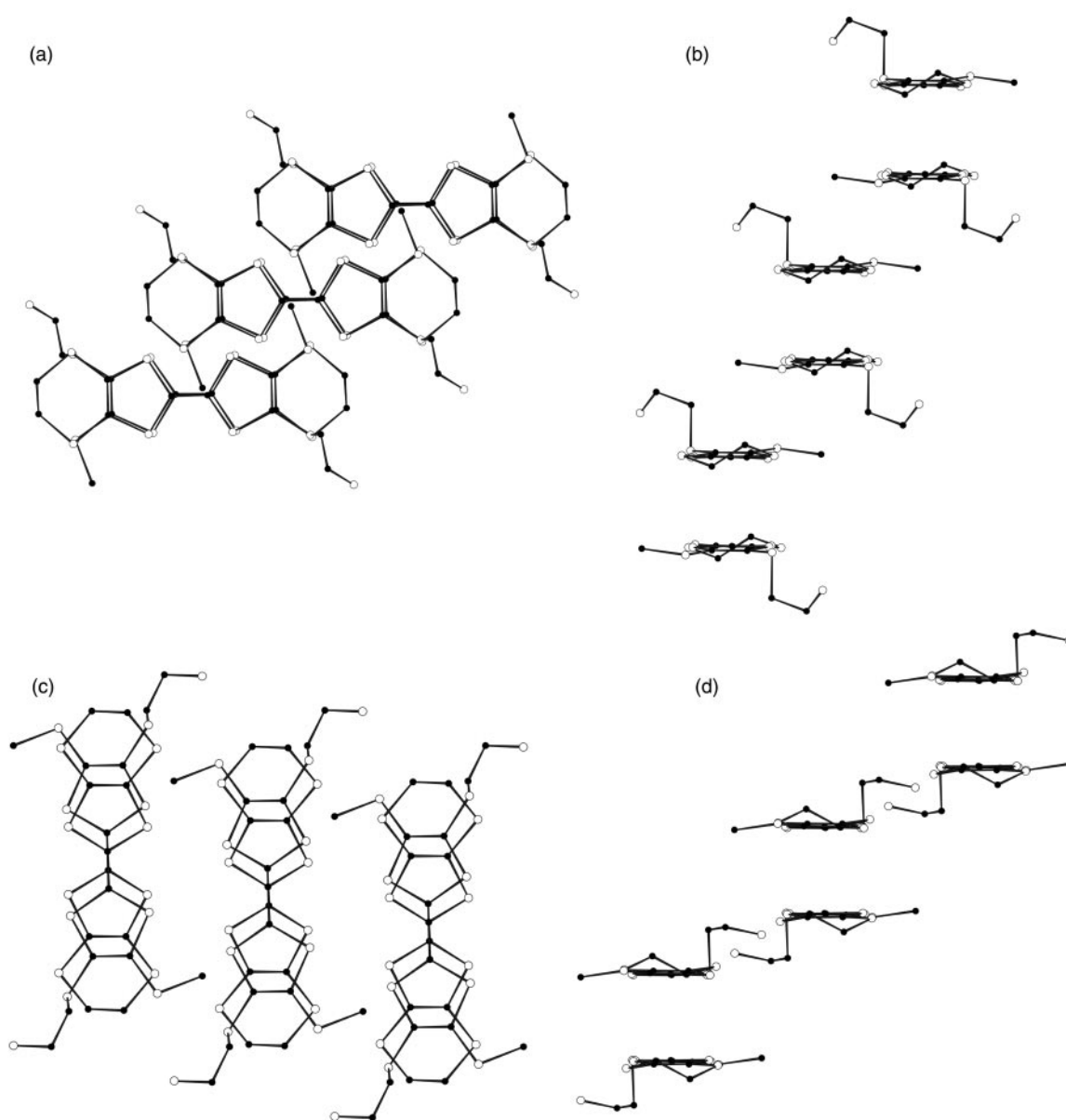


**Fig. 5** Comparison of the structure of the “stacks” in **9** and **9'**; three dimers are drawn. (a) and (c): projection onto a plane parallel to the molecular plane for **9** and **9'** respectively; (b) and (d): side view along the long molecular axis for **9** and **9'** respectively. Hydrogen atoms omitted for clarity.

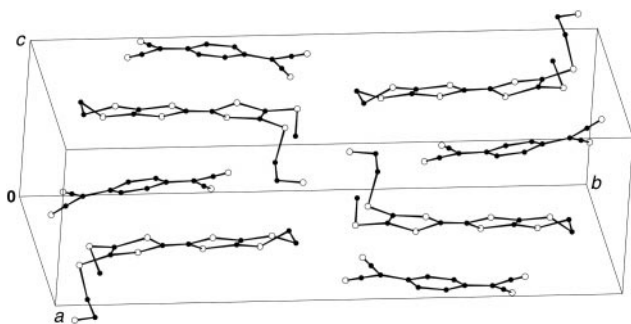


Fig. 6 Crystal structure of **11**. Hydrogen atoms omitted for clarity.

display overall packing features which are roughly similar. The cationic species are coupled head-to-tail to form centrosymmetric dimers which pile up to form “stacks”, but, within a “stack”, the dimers are strongly slipped with respect to each other both in the longitudinal and transverse directions (Fig. 5) in such a way that adjacent dimers do not overlap; this “staircase-like” arrangement is probably not favourable to electronic delocalization along the stacks. However, the two packings differ in details.

i – The two members of a dimer overlap in a different way in **9** and **9'**: in **9** the HETMT-EDTTTF entities overlap in a “TTF-core-over-TTF-core” manner, *i.e.* the two TTF cores are eclipsed when the dimer is projected onto the molecular plane (Fig. 5); on the other hand, in **9'** the two entities of a dimer are slipped in the longitudinal direction (Fig. 5) and this allows a shorter intradimer separation: the distance between the mean planes of the TTF cores within a dimer is 3.49 Å in **9** and 3.41 Å in **9'**.

ii – Within a “staircase” the relative positions of the dimers are strongly different in **9** and **9'** and can be characterized by three parameters: the estimated longitudinal and transverse offsets and the calculated interplanar separation, respectively 4.3 Å, 3.7 Å and 3.52 Å for **9** and 1 Å, 6 Å and 2.23 Å for **9'**; obviously, the short interplanar separation between two adjacent dimers in **9'** is possible only because of their large transverse offset.

iii – In both structures two adjacent “stacks” (or “stairs”) are related by the symmetry operators of the space group. Two angular parameters are well suited to describe the differences between the two phases: the angle between the long molecular axes of the entities of the two adjacent “stacks” is 89° in **9** and 93° in **9'** but the angles between the normals to the molecular planes are 12° in **9** and 76° in **9'** which indicates a quite different relative orientation of the molecular planes of the HETMT-EDTTTF entities in adjacent “stacks”.

iv – The ClO<sub>4</sub><sup>−</sup> anion is H-bonded to only one terminal –OH group in both structures, however, in **9**, only one oxygen atom takes part in H-bonding, while in **9'** two oxygen atoms are involved (Table 6) but the hydrogen bond involving O(3) is rather weak.

Complex **11** – The stoichiometry of this phase is 1 : 1 and its

low conductivity can easily be explained: the crystal structure is made of stacks in which the donor and acceptor molecules alternate in a ...D–A–D–A... pattern (Fig. 6). Using the criterion developed by Flandrois and Chasseau<sup>15</sup> and based on the bond lengths in TCNQ, the charge transfer can be roughly estimated to 0.8 electron.

## Conclusion

This study shows that the strategy which consists of functionalizing a TTF-like molecule with one or two hydroxylated side-chains, while preserving the good electron donating character of these TTF's as shown by cyclic voltammetry, is a two-edged sword: on the one hand, the flexibility of the side chain facilitates hydrogen bond formation, but, on the other hand the steric effects can hinder the formation of molecular stacking regular enough to allow electronic delocalisation. The compounds described in this paper suffer of this latter feature and display rather low conductivities. Thus new attempts should be made to grow systems with denser hydrogen bond networks.

## References

- 1 E. B. Yagubskii, *Mol. Cryst. Liq. Cryst.*, 1993, **230**, 139.
- 2 J. M. Williams, M. A. Beno, H. H. Wang, P. C. W. Leung, T. J. Enge, U. Geiser and K. D. Karlson, *Acc. Chem. Res.*, 1985, **18**, 261.
- 3 T. Ozturk, C. R. Rice and T. D. Wallis, *J. Mater. Chem.*, 1995, **5**(10), 1553.
- 4 G. J. Marshall, M. R. Bryce, G. Cooke, T. Jorgensen, J. Becher, C. D. Reynolds and S. Wood, *Tetrahedron*, 1993, **49**(31), 6849.
- 5 N. Svenstrup, K. M. Rasmussen, T. K. Hansen and T. Becher, *Synthesis*, 1994, 809; K. B. Simonsen, N. Svenstrup, J. Lau, O. Simonsen, P. Mork, G. T. Kristensen and J. Becher, *Synthesis*, 1996, 407.
- 6 L. Binet, J.-M. Fabre, C. Montginoul, K. B. Simonsen and J. Becher, *J. Chem. Soc., Perkin Trans. 1*, 1996, 783.
- 7 L. Binet, C. Montginoul, J.-M. Fabre, L. Ouahab, S. Golhen and J. Becher, *Synth. Met.*, 1997, **86**, 1825.
- 8 L. Binet and J.-M. Fabre, *Synthesis*, 1997, 1179.
- 9 J.-P. Legros, F. Dahan, L. Binet and J.-M. Fabre, *Synth. Met.*, 1999, **102**, 1632.
- 10 K. Bechgaard, K. Carneiro, F. B. Rasmussen and M. Olsen, *J. Am. Chem. Soc.*, 1981, **103**, 2440.
- 11 A. Altomare, G. Cascarano, C. Giacovazzo, A. Guagliardi, M. C. Burla, G. Polidori and M. Camalli, *J. Appl. Crystallogr.*, 1994, **27**, 435.
- 12 G. M. Sheldrick, SHELXS-86. Program for crystal structure solution, University of Göttingen, Göttingen, Germany, 1986.
- 13 D. J. Watkin, C. K. Prout, R. J. Carruthers and P. Betteridge, CRYSTALS, issue 10. Chemical Crystallography Laboratory, University of Oxford, Oxford, UK, 1996.
- 14 G. M. Sheldrick, SHELXL-93. Program for the refinement of crystal structures from diffraction data, University of Göttingen, Göttingen, Germany, 1993.
- 15 S. Flandrois and D. Chasseau, *Acta Crystallogr., Sect. B*, 1977, **33**, 2744.